

Angiogenesis versus Metabolic Imaging in Locally Advanced Breast Cancer Patients – A Comparative Study

Abstract

Purpose: The comparison of angiogenesis imaging (Ga-68-DOTA-Arginine-Glycine-Aspartic Acid [RGD]) positron emission tomography/computed tomography [PET/CT] with metabolic imaging (F-18 fluorodeoxyglucose [FDG] PET/CT) in primary staging and response assessment to neoadjuvant chemotherapy (NACT) in locally advanced breast cancer (LABC) patients. **Methods:** In this prospective study, 85 female patients with LABC were subjected to two PET/CT studies (Ga-68-DOTA-RGD₂ and F-18 FDG) within 1 week of each other. Thirty patients had repeat studies 4 weeks after completing eight cycles of NACT. Response assessment was done by RECIST 1.1 criteria. **Results:** Ga-68-DOTA-RGD₂ and F-18 FDG uptake in the primary tumor were seen in all patients. Ipsilateral axillary and internal mammary lymph nodes were detected in 77 (90.5%) versus 80 (94.1%) and 22 (25.8%) versus 27 (31.7%) patients on Ga-68-DOTA-RGD₂ and F-18 FDG scans, respectively. Ipsilateral supra-clavicular lymph nodes and skeletal lesions were noted in 17 (20%) versus 21 (24.7%) patients and 23 (27.0%) versus 24 (28.2%) patients on Ga-68-DOTA-RGD₂ versus F-18 FDG studies, respectively. However, the Ga-68-DOTA-RGD₂ did not show uptake in F-18 FDG avid liver lesions (LLs) in 10 patients, adrenal lesion in one patient, mediastinal lymph nodes in 2 patients, lung nodules, and pleural soft-tissue deposits, each in one patient. In response assessment, 23 and 25 patients had concordance with RECIST1.1 criteria on F-18 FDG and Ga-68-DOTA-RGD₂ scans, respectively. However, there were discordant results in four patients on Ga-68-DOTA-RGD₂ scan and two patients on F-18 FDG scans. **Conclusion:** Metabolic imaging is better in primary staging and chemotherapy response assessment than angiogenesis imaging in LABC patients. The latter may miss the metastatic soft-tissue deposits, adrenal, and LLs.

Keywords: Angiogenesis imaging, RGD (arg-gly-asp), F-18 FDG, Ga-68, locally advanced breast cancer

Introduction

Breast cancer is one of the significant reasons for cancer mortality in women.^[1] Accurate disease staging is a prerequisite to appropriate therapy and prediction of the prognosis for long-term survival. Locally advanced breast cancer (LABC) is defined as T0–T3 primary tumor with clinically evident ipsilateral axillary, ipsilateral infra-clavicular, supra-clavicular or internal mammary lymph nodes (IMLN) (N2–N3), or tumor involving chest wall or skin (T4) irrespective of the nodal status, corresponding to Stage III disease (T3 N1 M0, T0–T3 N2 M0, T4 N0–N2 M0, any T N3 M0). Numerous incidences of distant metastasis have been observed during the follow-up in LABC patients.^[2] Currently, neoadjuvant chemotherapy (NACT) along with surgery

and followed by radiotherapy is the choice in such patients. Hormonal therapy is also considered a crucial element of treatment regimen in a certain subgroup of LABC patients. However, despite the extensive primary treatment, the disease recurrence within 10 years is very high (up to 35%).^[3] The usefulness of fluorine-18 fluorodeoxyglucose (F-18 FDG) positron emission tomography (PET) imaging is well reported in breast cancer for staging, re-staging, treatment monitoring, prognostication and has been found to be more accurate and valuable to other present anatomic imaging modalities (computed tomography [CT], ultrasonography, magnetic resonance imaging, and X-rays).^[4-6] F-18 FDG PET has also been found superior to technetium-99 m methylene di-phosphonate (Tc-99 m MDP) bone scan in uncovering bony

Sunil Kumar,
Rakhee Vatsa,
Jaya Shukla,
Gurpreet Singh¹,
Amanjit Bal²,
Bhagwant Rai Mittal

Departments of Nuclear
Medicine, ¹General Surgery and
²Histopathology, Post Graduate
Institute of Medical Education
and Research, Chandigarh,
India

Address for correspondence:
Dr. Bhagwant Rai Mittal,
Department of Nuclear
Medicine, Post Graduate
Institute of Medical
Education and Research,
Chandigarh - 160 012, India.
E-mail: brmittal@yahoo.com

Received: 23-04-2021
Revised: 05-01-2022
Accepted: 07-01-2022
Published: 25-03-2022

Access this article online

Website: www.ijnm.in

DOI: 10.4103/ijnm.ijnm_53_21

Quick Response Code:



How to cite this article: Kumar S, Vatsa R, Shukla J, Singh G, Bal A, Mittal BR. Angiogenesis versus metabolic imaging in locally advanced breast cancer patients – A comparative study. Indian J Nucl Med 2022;37:54-60.

This is an open access journal, and articles are distributed under the terms of the Creative Commons Attribution-NonCommercial-ShareAlike 4.0 License, which allows others to remix, tweak, and build upon the work non-commercially, as long as appropriate credit is given and the new creations are licensed under the identical terms.

For reprints contact: WKHLRPMedknow_reprints@wolterskluwer.com

metastasis.^[7,8] However, it has limitations in detecting osteoblastic malignant skeletal lesions (SL).^[9-12]

Integrin $\alpha_v\beta_3$ plays an essential role in angiogenesis and distant metastasis. Low expression of $\alpha_v\beta_3$ integrin is observed on mature endothelial and epithelial cells. However, over expression of integrin $\alpha_v\beta_3$ has been reported on the activated endothelial cell of the neo-vasculature of the tumor. The restriction in the expression of $\alpha_v\beta_3$ integrin has an important part in tumor growth and invasion. This property makes integrin $\alpha_v\beta_3$ a valuable molecular target to help early diagnosis and management of various solid tumors, including breast, lung, and colorectal carcinoma.^[13-19]

Various radionuclides such as Tc-99 m, F-18, Copper-64 (Cu-64), and Gallium-68 (Ga-68) have been explored for radiolabeling of arginine-glycine-aspartic acid (RGD)-based peptide ligands targeting integrin $\alpha_v\beta_3$. However, the preparation of Ga-68 labeled RGD has attracted considerable interest for cancer imaging because of the ease of preparation and suitable physical characteristics of the radionuclide. The labeling chemistry of Ga-68 is facile and compatible with the pharmacokinetics of many peptides.^[20,21] The peptide ligands can also be radiolabeled with therapeutic radionuclides such as lutetium-177 (Lu-177), yttrium-90 (Y-90), and actinium-225 (Ac-225) to explore their therapeutic potential. The present study was carried out to compare the angiogenesis imaging using Ga-68 labeled DOTA-RGD₂ with metabolic imaging using F-18 FDG in primary staging and chemotherapy response assessment in LABC patients, along with assessing the future theranostic implications of RGD in treatment-refractory cases.

Materials and Methods

In this prospective study, a total of 85 female patients (mean age: 50 years, age range: 28–80 years) clinically diagnosed to have LABC were included. Each patient was subjected to 2 whole-body PET/CT scans (with Ga-68-DOTA-RGD₂ and F-18 FDG) before the start (in 85 patients) and after the completion (in 30 patients) of NACT. Both the studies were performed on two different days, within 1 week of each other, in random order. The Institutional Ethics Committee duly approved the study before recruiting patients (Approval no. Histopath/13/NK/2421, dated 08.12.2013). Written informed consent was obtained from each participant before enrolment.

At least 6 h of fasting and blood glucose level <200 mg/dL was ensured for the F-18 FDG study. Hybrid PET/CT images were acquired approximately 45 min after intravenous administration of F-18 FDG at a dose of 5 MBq/Kg body weight, using dedicated PET/CT scanners [Discovery 710 or Discovery STE-16, GE Healthcare, Milwaukee, USA]. Both oral and intravenous contrast agents were given in all F-18 FDG studies. Diagnostic CT images were acquired

first, followed by PET images in 6–7 bed positions (90 s per bed).

For Ga-68-DOTA-RGD₂ PET/CT, no special patient preparation was required. Images were acquired 40–45 min after slow intravenous injection of the radiotracer (2 MBq/Kg body weight). The image acquisition protocol used was similar to that of the F-18 FDG study. However, noncontrast low dose CT was performed instead, followed by PET images (6–7 bed positions) with each bed position for 120 s. Both the scans were acquired on the same PET/CT machine.

Data analysis

Data obtained from both the scans postattenuation correction were reconstructed using iterative reconstruction and ordered subset expectation maximization algorithm. The reconstructed images were displayed in transaxial, sagittal, and coronal views for qualitative and semi-quantitative evaluation. Two certified nuclear medicine physicians evaluated all the scans independently. Both the reviewers were blinded to the participant's clinical history and other parameters. For semi-quantitative assessment, standardized uptake value (SUV) estimation was done for uptake of Ga-68-DOTA-RGD₂ and F-18 FDG by drawing a circular region of interest over the entire lesion. It was expressed as SUV_{max (RGD)} and SUV_{max (FDG)}, respectively. The areas with increased focal uptake in the skeleton were considered malignant unless a benign cause, for example, degenerative bone disease was localized on corresponding CT images.

Response assessment was done as per RECIST 1.1 criteria.^[22] Complete disappearance, i.e., 100% decrease of the target lesion is considered as complete response (CR), 30% shrinkage in the longest diameter of the target lesion, as partial response (PR), 20% growth in the longest diameter of the target lesion as progressive disease (PD), and stable disease (SD)-neither PR nor PD. The response to chemotherapy (Δ SUV %) after eight cycles of chemotherapy was calculated as follows:

$$\Delta SUV (\%) = 100 \times (\text{Baseline SUV max} - \text{Posttherapy SUV max}) / \text{Baseline SUV max}$$

Histopathological assessment

Biopsy samples from patients were subjected to immunohistochemistry (IHC). Micro-vessel density (MVD) was calculated to assess the level of neo-angiogenesis and to see any correlation with SUV values of Ga-68-DOTA-RGD₂ and F-18 FDG.

Immunohistochemistry

IHC for endothelial cells was done using anti-CD31 antibody (Abcam, 1:50 dilution). Briefly, the sections of 4–5 μ m thickness were mounted on 0.01% poly-l-lysine coated slides. Xylene dewaxed sections were rehydrated in a series of graded alcohol and then washed in phosphate

buffer saline. The endogenous peroxidase activity was blocked with freshly prepared 0.03% hydrogen peroxide in methanol for 20 min. Antigen was recovered employing the heat retrieval method using PT link in citrate buffer (pH 5.9). Primary antibody was used on the sections for 1 h, followed by incubation with secondary antibody (Dako Envision) for 40 min. A coloured reaction was developed by Di-amino benzidine and counterstaining was done by using hematoxylin. The sections were then dehydrated and mounted with Dextrene Phthalate Xylene.

Micro-vessel density calculation

For microscope independent MVD values, counts were expressed as the number of microvessels/mm² (1 HPF = 0.17 mm²). Density counts of micro-vessels stained with CD31 were executed. Two independent investigators identified vascular “hot spots” at low power, and stained vessels were counted at x40 in at least five independent microscopic fields of each tissue section. MVD count was obtained by dividing the mean of five fields by the field area. For the proper delineation of tumor vasculature, vessel counting was avoided in the peripheral regions and was carried out at the center of the tumor.

Statistical analysis

Statistical analysis was carried out using a statistical package for social sciences (SPSS Inc., IBM, Chicago, Illinois, United States, version 23.0 for windows) software. The demographic profile of all participants was expressed in the form of descriptive statistics such as mean, standard deviation, and range. Both diagnostic methods were compared to each other for the number of skeletal, liver, or nodal metastasis, or metastasis to other sites (OS) both before (in 85 patients) and after completion (in 30 patients) of chemotherapy. For response prediction, the threshold SUV change was calculated by using receiver-operating characteristic (ROC) analysis. Correlation between the paired variables was done using Spearman's Rho. $P < 0.05$ was considered statistically significant.

Results

Baseline study

Both Ga-68-DOTA-RGD₂ and F-18 FDG show good uptake at the primary tumor site in all 85 patients with mean SUV_{max (RGD)} 6.7 ± 3.1 (range 2.5–20.7) and mean SUV_{max (FDG)} 13.1 ± 5.9 (range 3.4–32.0). Regional lymph nodes (ipsilateral axillary lymph nodes and ipsilateral IMLN) were Ga-68-DOTA-RGD₂ avid in 77 (90.5%) and 22 (25.8%) patients and F-18 FDG avid in 80 (94.1%) and 27 (31.7%) patients. Contralateral axillary lymph nodes (CALN) were found in 10 (11.7%) versus 11 (12.9%) patients on Ga-68-DOTA-RGD₂ versus F-18 FDG study, respectively. Ipsilateral supra-clavicular lymph nodes (ISCL) were seen in 17 (20%) versus 21 (24.7%) patients on Ga-68-DOTA-RGD₂ versus F-18 FDG scans, respectively, as shown in Figure 1. A total of 10 patients

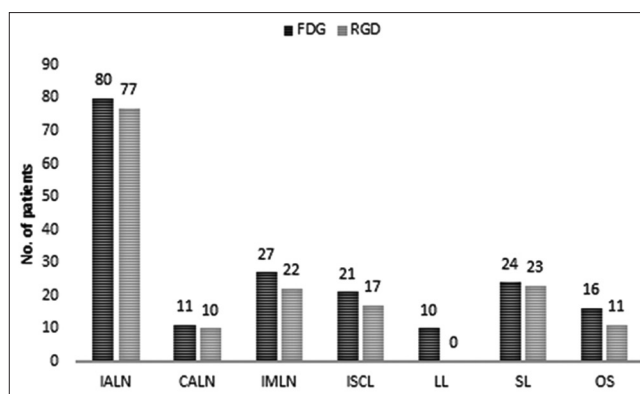


Figure 1: Bar chart showing pre chemotherapy findings on F-18 fluorodeoxyglucose positron emission tomography/computed tomography and Ga-68-DOTA-RGD₂. IALN: Ipsilateral axillary lymph node, CALN: Contralateral axillary lymph node, IMLN: Ipsilateral internal mammary lymph node, ISCL: Ipsilateral supraclavicular lymph node, LL: Liver lesion, SL: Skeletal lesion, OS: Other sites (brain lesion, contralateral breast lesion, lung nodules, pleural deposit, mediastinal and abdominal lymph node and adrenal lesion)

with hypo-attenuating liver lesions (LLs) on CT images showed F-18 FDG uptake, but none revealed avidity for RGD. Lytic SLs were Ga-68-DOTA-RGD₂ avid in 23 (27.0%) patients and F-18 FDG avid in 24 (28.2%) patients [Figure 2]. Lesions at OS, i.e., brain, contralateral breast, and adrenal lesions, lung nodules, pleural deposits, mediastinal, and abdominal lymph nodes were detected in 11 versus 16 patients on Ga-68-DOTA-RGD₂ and F-18 FDG study, respectively.

The direct comparison of PET/CT findings using these two tracers reveals that both could identify contralateral breast lesions (two patients; with supra-clavicular lymph nodes in one patient), lung nodules (six patients), mediastinal and abdominal lymph nodes (in 2 and 3 patients, respectively), and brain lesion (1 patient). However, lymph nodes in mediastinum, lung nodules, and adrenal lesion each in one patient were F-18 FDG avid, whereas Ga-68-DOTA-RGD₂ did not show any uptake in these lesions. M stage was changed from Mx to M1 in 31 (36.5%) patients on Ga-68-DOTA-RGD₂ and 38 (44.7%) on F-18 FDG studies.

The lesion wise analysis of both radiotracers is shown in Table 1. A total of 1156 lesions were identified on F-18 FDG PET/CT and out of these, 1070 lesions also showed avidity for Ga-68-DOTA-RGD₂. A total of 86 lesions did not show Ga-68-DOTA-RGD₂ uptake, mainly 44 LLs, five pleural deposits and one adrenal lesion.

Micro-vessel density correlation

MVD was calculated in 62 patients with anti-CD31 IHC in core biopsy samples from the primary tumor [Figure 3]. Mean MVD count was 110.1 ± 35.3 . No statistically significant correlation of MVD was seen either with SUV_{max (RGD)} or SUV_{max (FDG)}. Spearman's correlation coefficient values were 0.08 for SUV_{max (RGD)} and 0.088 for SUV_{max (FDG)} respectively [Table 2].

Table 1: Lesion-wise analysis of Ga-68-DOTA-RGD₂ and F-18 fluorodeoxyglucose

Number of lesions	RGD positive	FDG positive	Concordant	Discordant
Primary (including satellite nodules)	145	145	145	0
IALN	443	447	443	4
CALN	39	40	39	1
IMLN	45	54	45	9
ISCL	55	65	55	10
LL	0	44	0	44
SL	266	267	266	1
Contralateral breast lesion	2	2	2	0
Lung nodules	40	42	40	2
Mediastinal lymph nodes	21	30	21	9
Pleural deposits	0	5	0	5
Abdominal lymph nodes	13	13	13	0
Brain lesion	1	1	1	0
Adrenal lesion	0	1	0	1
Total number of lesions	1070	1156	1070	86

IALN: Ipsilateral axillary lymph node, IMLN: Ipsilateral internal mammary, CALN: Contralateral axillary lymph node, ISCL: Ipsilateral supra-clavicular lymph, LL: Liver lesion, SL: Skeletal lesion, RGD: Ga-68-DOTA-RGD₂

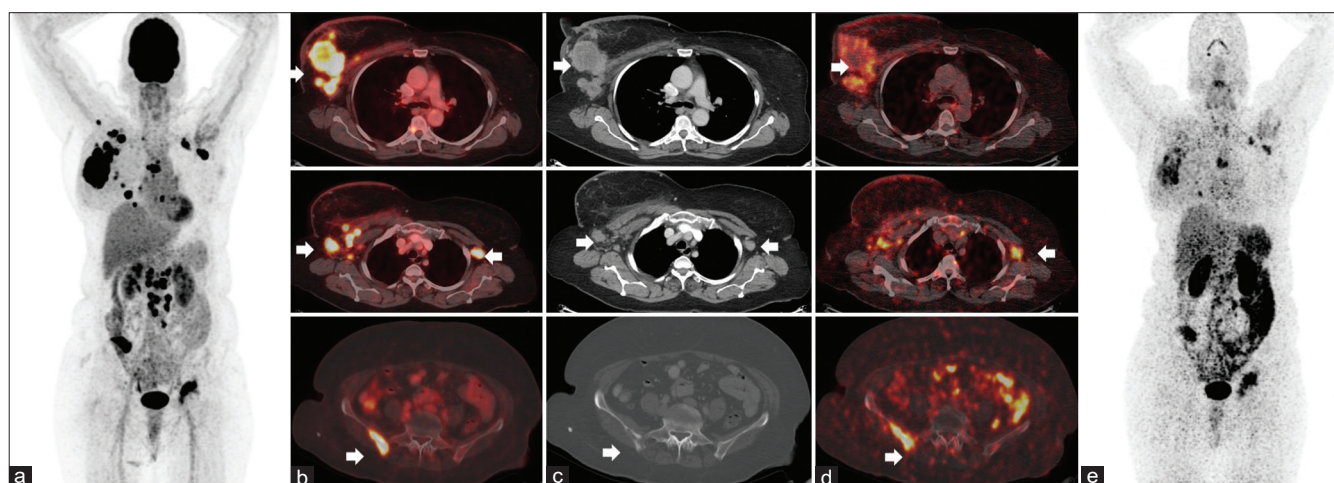


Figure 2: A 65-year-old female with locally advanced breast cancer referred for initial evaluation: (a) MIP image of F-18 fluorodeoxyglucose positron emission tomography/computed tomography, (b) fused transaxial F-18 fluorodeoxyglucose positron emission tomography/computed tomography sections, (c) computed tomography sections and (d) transaxial fused Ga-68-DOTA-RGD₂ positron emission tomography/computed tomography images (e) MIP image of Ga-68-DOTA-RGD₂ positron emission tomography/computed tomography. In the top row, F-18 fluorodeoxyglucose and Ga-68-DOTA-RGD₂ uptake is noted in primary tumor in the right breast. In middle row uptake of both tracers is seen in ipsilateral and contralateral axillary lymph nodes. Bottom row showing uptake of both tracers in lytic lesion in the right iliac bone

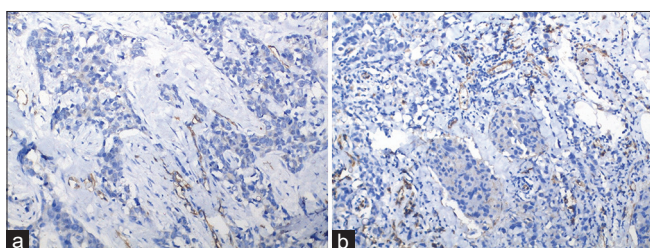


Figure 3: Microphotographs showing micro-vessels highlighted by CD31 immunostain (a) ×10 image (b) ×40 image

Postchemotherapy study

A total of 30 patients have undergone both Ga-68-DOTA-RGD₂ and F-18 FDG PET/CT 4 weeks postcompletion of eight cycles of chemotherapy. In

10 patients, complete resolution of the primary tumor was seen, and in the rest of 20 patients, both the tracers showed a decrease in the uptake with mean SUVmax_(RGD) 3.42 ± 0.74 and mean SUVmax_(FDG) 3.2 ± 0.59 , respectively, suggesting residual primary tumor [Figure 4]. In the posttherapy scans, nine of these 30 patients showed Ga-68-DOTA-RGD₂ and F-18 FDG avid residual ipsilateral axillary lymph nodes. SL (7/30 patients), ipsilateral internal mammary (3/30 patients), ISCL (2/30 patients) also showed radiotracer uptake in both the scans. One patient with LL and another with pleural lesions showed F-18 FDG uptake but no Ga-68-DOTA-RGD₂ uptake in the posttherapy scans. No lymph nodes in the contralateral axilla were detected in any patient on both scans. Lung nodules were noted in one patient on both scans.

Response assessment

The response to chemotherapy was evaluated by RECIST 1.1 criteria. Twenty-seven patients showed favorable response to chemotherapy. CR was noted in 10 of these 27 patients and PR in 17 patients. In nonresponder category, two patients had stable SD while one showed PD.

Determination of Δ standardized uptake value (%) threshold

For differentiation of responders (CR or PR) and nonresponders (SD or PD) after completion of chemotherapy, ROC analysis indicated Δ SUV(%) threshold of 35% (sensitivity of 80% and specificity of 75%) for Ga-68-DOTA-RGD₂ and 45% (sensitivity of 92% and specificity of 75%) for F-18 FDG [Figure 5]. Based on these cutoffs, seven patients were labeled as nonresponders on Ga-68-DOTA-RGD₂ and five on F-18 FDG [Table 3]. In nonresponder group, three patients had concordance with RECIST 1.1 criteria and both Ga-68-DOTA-RGD₂ and F-18 FDG scan findings while two patients on F-18 FDG and four patients on Ga-68-DOTA-RGD₂ had discordant results. In responder group, in comparison to RECIST 1.1 criteria, 23 and 25 patients had concordance with Ga-68-DOTA-RGD₂ and F-18 FDG scans, respectively.

However, discordant results were observed in four patients on Ga-68-DOTA-RGD₂ and in two patients on F-18 FDG scan.

Table 2: Correlation of micro-vessel density with maximum standardized uptake value of RGD and FDG

	SUVmax _(RGD)	SUVmax _(FDG)
Spearman's rho coefficient	-0.080	0.088
P*	0.54	0.5

*P_≤0.05 is significant. MVD: Micro-vessel density, SUVmax: Maximum standardized uptake value, RGD: Ga-68-DOTA-RGD₂

Table 3: Response assessment, comparison between RECIST 1.1 and positron emission tomography

	RECIST 1.1	PET criteria	
		RGD	FDG
Responders (CR/PR)	27 (10/17)	23 (10/13)	25 (10/15)
Non responders (SD/PD)	3 (2/1)	7 (6/1)	5 (4/1)

Response assessment based on Δ SUV (%) cut-off of 45% and 35% for FDG and RGD respectively. CR: Complete response, PR: Partial response, SD: Stable disease, PD: Progressive disease, FDG: Fluorodeoxyglucose, PET: Positron emission tomography, RGD: Ga-68-DOTA-RGD₂

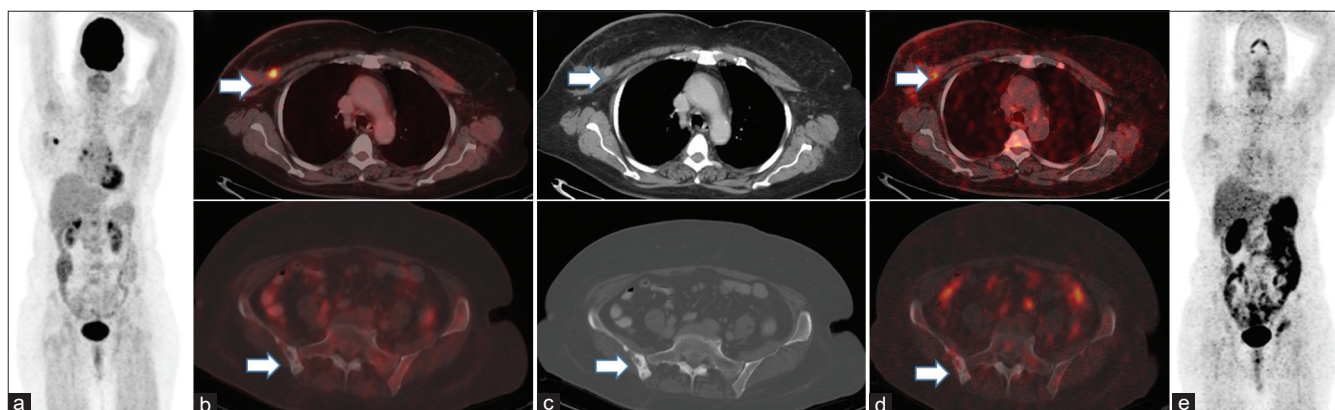


Figure 4: Patient in Figure 2 after eight cycles of chemotherapy: (a) MIP image of F-18 FDG PET/CT, (b) fused transaxial F-18 fluorodeoxyglucose positron emission tomography/computed tomography sections, (c) computed tomography sections (d) transaxial fused Ga-68-DOTA-RGD₂ PET/CT images and (e) MIP image of Ga-68-DOTA-RGD₂. In top row F-18 FDG and Ga-68-DOTA-RGD₂ uptake is noted in residual primary tumor in right breast. Bottom row showing lytic-sclerotic lesion, with no uptake of either F-18 fluorodeoxyglucose or Ga-68-DOTA-RGD₂

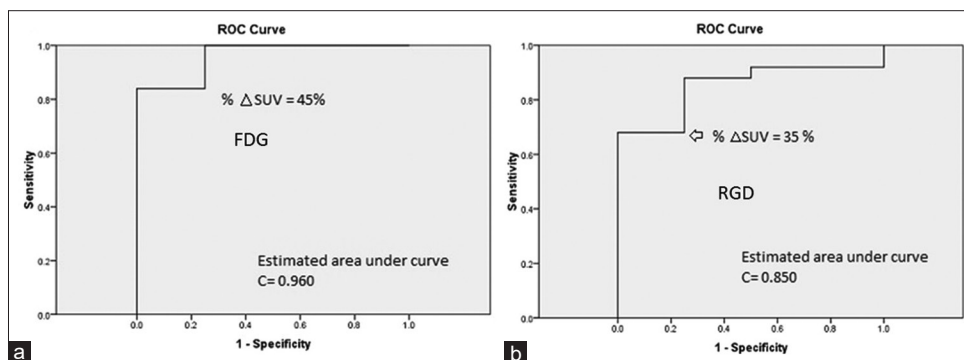


Figure 5: (a) ROC analysis curve, establishing optimal cutoff values of Δ SUV (%) for F-18 FDG, (b) ROC analysis curve, establishing optimal cutoff values of Δ SUV (%) for Ga-68-DOTA-RGD₂

Discussion

The diagnosis at the early stage of the disease in breast cancer makes cure possible. Imaging modalities that could detect disease early and identify regional and distant disease spread help plan the management.^[23]

F-18 FDG PET is a highly sensitive modality for illustrating lymph nodal disease (sub-and inter-pectoral disease, supra-and intra-clavicular and internal mammary chain) and other metastatic lesions in breast cancer. However, it lacks specificity due to its uptake in infectious/inflammatory conditions and reactive lymph nodal hyperplasia, which must be confirmed histologically.^[24] In the present study, both Ga-68-DOTA-RGD₂ and F-18 FDG studies were equally sensitive for the detection of primary tumor; however, F-18 FDG was observed to be more sensitive in the evaluation of disease spread to regional lymph nodes.

Distant metastasis in a patient precludes the radical surgery and needs to be managed with palliative chemotherapy or radiotherapy. Both radiotracers Ga-68-DOTA-RGD₂ and F-18 FDG are useful to uncover distant metastases. In our study, comprising clinically suspected LABC patients, 31/85 patients (36.5%) on Ga-68-DOTA-RGD₂ and 38/85 (44.7%) patients on F-18 FDG scans, were upstaged from M0 to M1. Skeletal metastasis (osteolytic lesions) was seen in 23 versus 24 patients on Ga-68-DOTA-RGD₂ versus F-18 FDG study. However, RGD expression was not seen in any metastatic LLs [Figure 6]. Similar observations showing the inability of RGD peptides to detect hepatocellular carcinoma and metastatic LLs have been reported earlier. However, the exact reason was not ruled out.^[25,26] OS of metastasis were CALN, contralateral breast lesions, lung nodules, pleural soft-tissue deposits, mediastinal and abdominal lymphadenopathy, adrenal gland and brain lesions. All these lesions were detected by F-18 FDG study, but Ga-68-DOTA-RGD₂ did not show any uptake in pleural soft-tissue deposits, lung nodule and mediastinal lymph nodes (each in 1 patient). This needs further investigation in future studies with larger patient population.

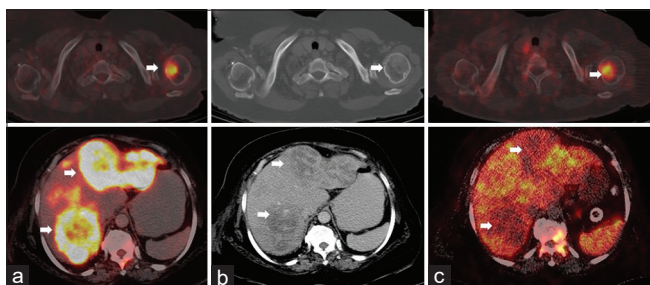


Figure 6: A 64-year-old female with locally advanced breast cancer referred for initial evaluation. (a) Transaxial fused F-18 fluorodeoxyglucose positron emission tomography/computed tomography images, (b) computed tomography images and (c) transaxial fused Ga-68-DOTA-RGD₂ positron emission tomography/computed tomography images. Top row showing F-18 fluorodeoxyglucose and Ga-68-DOTA-RGD₂ avid lytic lesion in head of left humerus. In bottom row, multiple fluorodeoxyglucose avid hypo-dense liver lesions are seen which are not avid on Ga-68-DOTA-RGD₂

Another focus of this study was response assessment to NACT. In the responder group, concordance was noted between RECIST 1.1 and Δ SUV (%) threshold values of F-18 FDG in 25 patients and Ga-68-DOTA-RGD₂ in 23 patients. In both the studies, CR was observed in total of 10 patients. In the nonresponder group, good agreement between RECIST 1.1 and Δ SUV (%) threshold values (of both tracers) was observed in 3 patients.

High expression of integrin $\alpha_v\beta_3$ has been reported on activated endothelial cells and tumor cells. The role of $\alpha_v\beta_3$ integrin in regulating tumor growth and distant metastasis is well known. Previous preclinical and clinical studies have demonstrated the correlation between $\alpha_v\beta_3$ expression in tumor and uptake of radiolabeled RGD peptides.^[27,28] Expression of $\alpha_v\beta_3$ could not be evaluated in this study due to some technical reasons; however, the MVD was evaluated by CD31 expression to demonstrate neo-angiogenesis in pretherapy biopsy samples. MVD results did not correlate with either SUVmax_(RGD) or SUVmax_(FDG) values in this study. The possible reason could be that the core biopsy samples were not guided by Ga-68-DOTA-RGD₂ or F-18 FDG uptake in the primary tumor.

The synthesis of Ga-68-DOTA-RGD₂ is facile providing good yield. Moreover, patients who are nonresponsive to neo-adjuvant chemotherapy and have advanced disease may in future be candidates for radionuclide therapy using ¹⁷⁷Lu-⁹⁰Y-RGD.

Conclusion

F-18 FDG appears better tracer for primary staging and chemotherapy response assessment than Ga-68-DOTA-RGD₂ in LABC patients. Further RGD peptide also missed metastatic LL, pleural deposits, and adrenal lesion.

Declaration of patient consent

The authors certify that they have obtained all appropriate patient consent forms. In the form the patient (s) has/have given his/her/their consent for his/her/their images and other clinical information to be reported in the journal. The patients understand that their names and initials will not be published and due efforts will be made to conceal their identity, but anonymity cannot be guaranteed.

Financial support and sponsorship

Nil.

Conflicts of interest

There are no conflicts of interest.

References

- Greenlee RT, Murray T, Bolden S, Wingo PA. Cancer statistics, 2000. *CA Cancer J Clin* 2000;50:7-33.
- Perez EA, Foo ML, Fulmer JT. Management of locally advanced breast cancer. *Oncology (Williston Park)* 1997;11:9-17.

3. van Dongen JA, Voogd AC, Fentiman IS, Legrand C, Sylvester RJ, Tong D, *et al.* Long-term results of a randomized trial comparing breast-conserving therapy with mastectomy: European Organization for Research and Treatment of Cancer 10801 trial. *J Natl Cancer Inst* 2000;92:1143-50.
4. Avril N, Rosé CA, Schelling M, Dose J, Kuhn W, Bense S, *et al.* Breast imaging with positron emission tomography and fluorine-18 fluorodeoxyglucose: Use and limitations. *J Clin Oncol* 2000;18:3495-502.
5. Mittal BR, Manohar K, Kashyap R, Bhattacharya A, Singh B, Singh G. The role of (18) F-FDG PET/CT in initial staging of patients with locally advanced breast carcinoma with an emphasis on M staging. *Hell J Nucl Med* 2011;14:135-9.
6. Suárez M, Pérez-Castejón MJ, Jiménez A, Domper M, Ruiz G, Montz R, *et al.* Early diagnosis of recurrent breast cancer with FDG-PET in patients with progressive elevation of serum tumor markers. *Q J Nucl Med* 2002;46:113-21.
7. Tatsumi M, Cohade C, Mourtzikos KA, Fishman EK, Wahl RL. Initial experience with FDG-PET/CT in the evaluation of breast cancer. *Eur J Nucl Med Mol Imaging* 2006;33:254-62.
8. Fueger BJ, Weber WA, Quon A, Crawford TL, Allen-Auerbach MS, Halpern BS, *et al.* Performance of 2-deoxy-2-[F-18]fluoro-D-glucose positron emission tomography and integrated PET/CT in restaged breast cancer patients. *Mol Imaging Biol* 2005;7:369-76.
9. Huyge V, Garcia C, Vanderstappen A, Alexiou J, Gil T, Flamen P. Progressive osteoblastic bone metastases in breast cancer negative on FDG-PET. *Clin Nucl Med* 2009;34:417-20.
10. Nakai T, Okuyama C, Kubota T, Yamada K, Ushijima Y, Taniike K, *et al.* Pitfalls of FDG-PET for the diagnosis of osteoblastic bone metastases in patients with breast cancer. *Eur J Nucl Med Mol Imaging* 2005;32:1253-8.
11. Cook GJ, Houston S, Rubens R, Maisey MN, Fogelman I. Detection of bone metastases in breast cancer by 18FDG PET: Differing metabolic activity in osteoblastic and osteolytic lesions. *J Clin Oncol* 1998;16:3375-9.
12. Cook GJ, Fogelman I. The role of positron emission tomography in skeletal disease. *Semin Nucl Med* 2001;31:50-61.
13. Clezardin P. Recent insights into the role of integrins in cancer metastasis. *Cell Mol Life Sci* 1998;54:541-8.
14. Eliceiri BP, Cheresh DA. The role of alphav integrins during angiogenesis: Insights into potential mechanisms of action and clinical development. *J Clin Invest* 1999;103:1227-30.
15. Cox D, Aoki T, Seki J, Motoyama Y, Yoshida K. The pharmacology of the integrins. *Med Res Rev* 1994;14:195-228.
16. Brooks PC, Strömblad S, Klemke R, Visscher D, Sarkar FH, Cheresh DA. Antiintegrin alpha v beta 3 blocks human breast cancer growth and angiogenesis in human skin. *J Clin Invest* 1995;96:1815-22.
17. Takayama S, Ishii S, Ikeda T, Masamura S, Doi M, Kitajima M. The relationship between bone metastasis from human breast cancer and integrin alpha(v) beta3 expression. *Anticancer Res* 2005;25:79-83.
18. Furger KA, Allan AL, Wilson SM, Hota C, Vantuyghem SA, Postenka CO, *et al.* Beta (3) integrin expression increases breast carcinoma cell responsiveness to the malignancy-enhancing effects of osteopontin. *Mol Cancer Res* 2003;1:810-9.
19. Vellon L, Menendez JA, Liu H, Lupu R. Up-regulation of alphavbeta3 integrin expression is a novel molecular response to chemotherapy-induced cell damage in a heregulin-dependent manner. *Differentiation* 2007;75:819-30.
20. Dijkgraaf I, Yim CB, Franssen GM, Schuit RC, Luurtsema G, Liu S, *et al.* PET imaging of $\alpha v \beta_3$ integrin expression in tumours with ^{68}Ga -labelled mono-, di- and tetrameric RGD peptides. *Eur J Nucl Med Mol Imaging* 2011;38:128-37.
21. Vatsa R, Ashwathanarayana AG, Shukla J, Singh S, Bhusari P, Kumar R, *et al.* Multifarious Ga-68 labeled PET radiopharmaceuticals in imaging various malignancies. *Indian J Nucl Med* 2018;33:242-4.
22. Eisenhauer EA, Therasse P, Bogaerts J, Schwartz LH, Sargent D, Ford R, *et al.* New response evaluation criteria in solid tumours: Revised RECIST guideline (version 1.1). *Eur J Cancer* 2009;45:228-47.
23. Kumar R, Alavi A. Fluorodeoxyglucose-PET in the management of breast cancer. *Radiol Clin North Am* 2004;42:1113-22.
24. Groheux D, Moretti JL, Baillet G, Espie M, Giacchetti S, Hindie E, *et al.* Effect of (18) F-FDG PET/CT imaging in patients with clinical Stage II and III breast cancer. *Int J Radiat Oncol Biol Phys* 2008;71:695-704.
25. Haubner R, Finkenstedt A, Stegmayr A, Rangger C, Decristoforo C, Zoller H, *et al.* [68Ga] NODAGA-RGD—Metabolic stability, biodistribution, and dosimetry data from patients with hepatocellular carcinoma and liver cirrhosis. *Eur J Nucl Med Mol Imaging* 2016;43:2005-13.
26. Kenny LM, Coombes RC, Oulie I, Contractor KB, Miller M, Spinks TJ, *et al.* Phase I trial of the positron-emitting Arg-Gly-Asp (RGD) peptide radioligand 18F-AH111585 in breast cancer patients. *J Nucl Med* 2008;49:879-86.
27. Beer AJ, Niemeier M, Carlsen J, Sarbia M, Nährig J, Watzlowik P, *et al.* Patterns of alphavbeta3 expression in primary and metastatic human breast cancer as shown by 18F-Galacto-RGD PET. *J Nucl Med* 2008;49:255-9.
28. Vatsa R, Shukla J, Kumar S, Chakraborty S, Dash A, Singh G, *et al.* Effect of macro-cyclic bifunctional chelators DOTA and NODAGA on radiolabeling and *in vivo* biodistribution of Ga-68 cyclic RGD dimer. *Cancer Biother Radiopharm* 2019;34:427-35.